

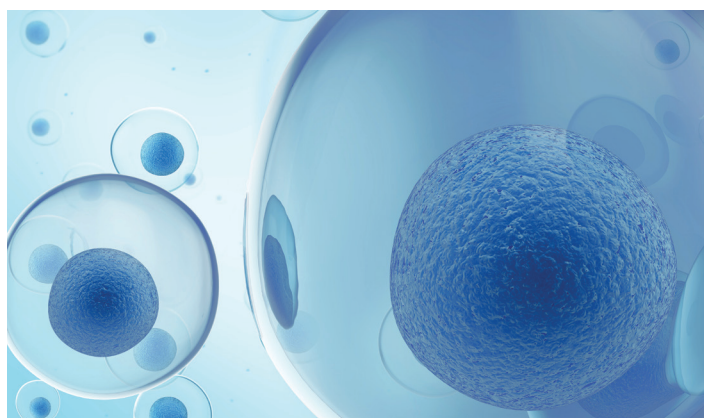
Advanced ICP-MS techniques for overcoming interferences in LA-ICP-MS bioimaging

Authors: Georgina M. Thyssen¹, Michael Sperling^{1,2}, Uwe Karst¹, Christoph A. Wehe³ and Julian D. Wills³;
¹Institute of Inorganic and Analytical Chemistry, University of Münster, Corrensstr. 28/30, 48149 Münster, Germany; ²European Virtual Institute for Speciation Analysis, Mendelstr. 11, 48149 Münster, Germany; ³Thermo Fisher Scientific (Bremen) GmbH, Hanna-Kunath-Straße 11, 28199 Bremen, Germany

Keywords: LA-ICP-MS, bioimaging, triple quadrupole ICP-MS

Goal

To highlight image contrast improvements achieved by triple quadrupole ICP-MS over single quadrupole ICP-MS for Laser Ablation bioimaging analyses due to enhanced interference removal.



Introduction

In recent years, an increasing number of studies in the field of Life Sciences – especially Metallomics – have been published that employ different imaging techniques to, for example, understand the fundamental principles of cancer growth or illuminate the importance of the availability or absence of different (trace) elements in crop production. For trace and ultratrace elemental analysis, laser ablation inductively coupled plasma mass spectrometry (LA-ICP-MS) has become one of the methods of choice due to its high sensitivity, linearity over several orders of magnitude and the possibility for quantitation. One of the major challenges, however, is the presence of isobaric and polyatomic interferences leading to false positive results. This is especially important for the transient signals produced by LA-ICP-MS, where it is hard to predict if the signal is affected by interferences.

Chemical resolution, i.e. the utilization of selective mass shift reactions performed on the analyte or plasma-based interferences using triple quadrupole ICP-MS (Thermo Scientific™ iCAP™ TQ ICP-MS), can be used to improve analytical figures of merit for difficult elements such as iron, selenium, phosphorus and others. This is of particular importance for bioimaging samples, which often consist of thin sections and need to be analyzed at high spatial resolution, leading to only minute amounts of sample being introduced into the plasma per laser shot.

Instrumentation

For the analysis, a Teledyne CETAC Technologies LSX-213 G2+ laser ablation system was coupled to an iCAP TQ ICP-MS. The iCAP TQ ICP-MS was configured with a high sensitivity interface (Table 1) to ensure the detection of analytes even in low concentrations and small amounts of ablated sample. Prior to the measurements, all plasma and interface related settings were tuned automatically and were fully tailored to the LA-based sample introduction by using the autotune procedures provided in the Thermo Scientific Qtegra™ Intelligent Scientific Data Solution (ISDS) Software. For the analysis, three different measurement modes were applied:

SQ-O₂ – single quadrupole mode with collision/reaction cell (CRC) pressurized with oxygen as reaction gas.

SQ-KED – single quadrupole mode with CRC pressurized with helium as a collision gas and Kinetic Energy Discrimination (KED) applied.

TQ-O₂ – triple quadrupole mode with CRC pressurized with oxygen as a reaction gas, first quadrupole (Q1) set to analyte mass (M⁺) and third quadrupole (Q3) set to product ion mass (MO⁺).

Table 1. Instrument parameters for LA-ICP-MS measurements

Parameter	Value
ICP-MS Parameter	
System	Thermo Scientific iCAP TQ ICP-MS
Injector	2.5 mm i.d., quartz
Interface	Ni cones with High Sensitivity (2.8 mm) insert
RF Power	1,550 W
CRC Gas Flow	TQ-O ₂ & SQ-O ₂ : 0.4 mL·min ⁻¹ O ₂ SQ-KED: 5.1 mL·min ⁻¹ He
Autotune	Laser ablation interface Tune using NIST 612 glass standard
LA Parameter	
System	Teledyne CETAC Technologies LSX-213 G2+ Laser Ablation System
Ablation Cell	HelEx II cell for fast wash-out
Spotsize	25 μm
Scan Speed	75 μm·s ⁻¹
Energy	4.5 J·m ⁻²
Ablation Cell Gas Flow	0.8 L·min ⁻¹ He
Makeup Gas Flow	1 L·min ⁻¹ Ar (added behind the ablation cell)

Sample preparation

Tobacco stems and petioles were embedded in hydroxyethyl cellulose (an embedding medium with low Ca content), frozen and cryosectioned into 30 μm thin sections. They were then transferred onto quartz glass sample mounts (also with lower Ca background than usual borosilicate glass sample mounts).

Rat kidneys were embedded into Technovit® and sectioned into 5 μm thin sections. Subsequently, they were transferred onto glass sample mounts.

Rat livers were frozen, cryosectioned into 5 μm thin sections and transferred onto glass sample mounts.

Results – Comparison of SQ and TQ modes for the analysis of tobacco petioles

For plant samples such as tobacco (*Nicotiana tabacum*), nutritional elements are analytes of high interest. One of these elements is Ca, which contributes to plant wound sealing and defence and is crucial for signal transduction in eukaryotic cells in general. Changes in the calcium distribution across growth stages or differences between wild types and genetically modified plants can give valuable information about all these mechanisms. Even though LA-ICP-MS is a powerful tool for bioimaging, access to calcium by SQ-ICP-MS is complicated by both background gas interferences (e.g. $^{40}\text{Ar}^+$ on $^{40}\text{Ca}^+$, $^{40}\text{Ar}^4\text{He}^+$ on $^{44}\text{Ca}^+$) as well as those generated by the sample matrix (e.g. $^{39}\text{K}^1\text{H}^+$ on $^{40}\text{Ca}^+$).

Phosphorous and sulphur are used for visualization in many biological samples as they are present in all living cells and provide clear structural information. They are, however, difficult to access via traditional SQ-ICP-MS due to the presence of intense interferences from background (gas) species (e.g. $^{16}\text{O}^{16}\text{O}^+$ on $^{32}\text{S}^+$).

For comparison of single quadrupole and triple quadrupole performance, a tobacco petiole thin section (Figure 1) was analyzed in SQ- O_2 mode (right half of the petiole, Figure 2) and TQ- O_2 mode (left half of the same petiole, Figure 3). To avoid interferences in both modes, a mass shift reaction with oxygen has been applied to all three analytes ($^{31}\text{P} \rightarrow ^{31}\text{P}^{16}\text{O}$, $^{32}\text{S} \rightarrow ^{32}\text{S}^{16}\text{O}$, $^{44}\text{Ca} \rightarrow ^{44}\text{Ca}^{16}\text{O}$).

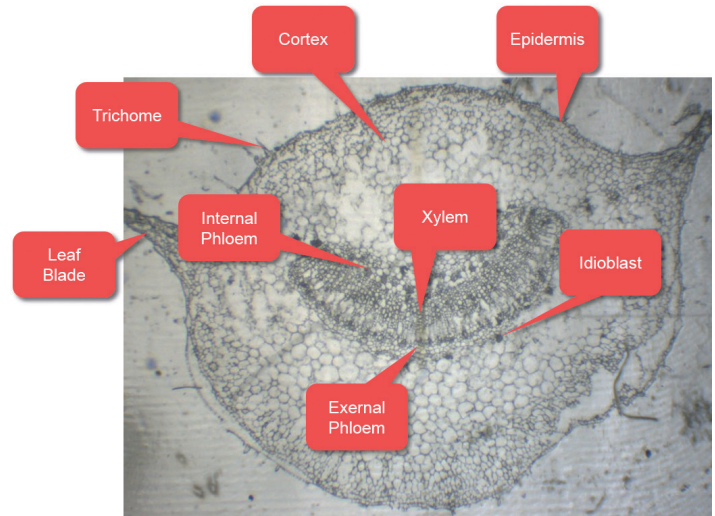


Figure 1. Visible light image of a thin section from a tobacco petiole, indicating major structures

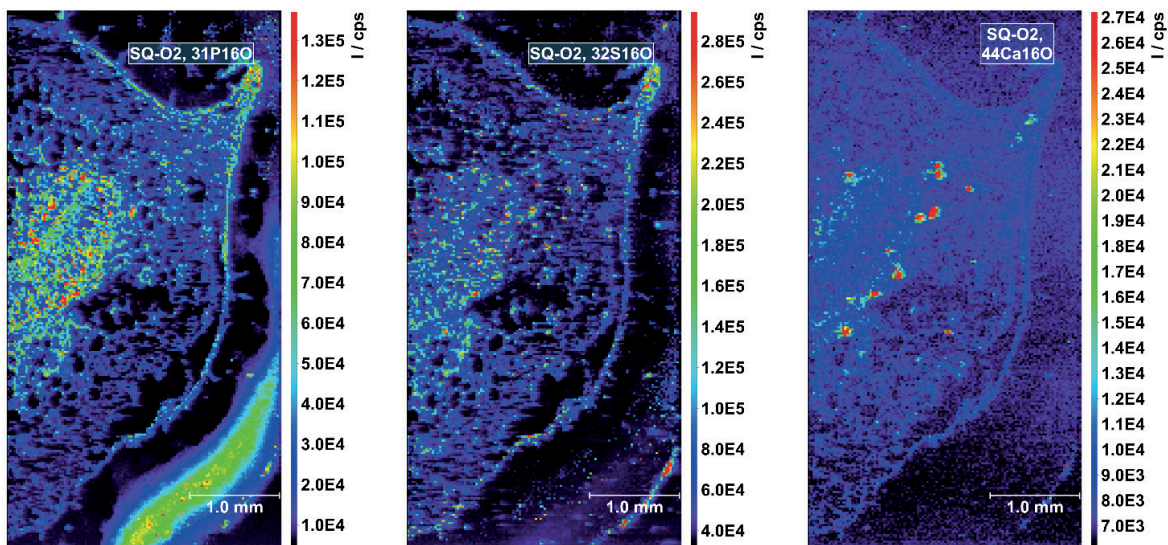


Figure 2. Elemental distribution maps for the SQ- O_2 analysis of $^{31}\text{P}^{16}\text{O}$ (left), $^{32}\text{S}^{16}\text{O}$ (middle) and $^{44}\text{Ca}^{16}\text{O}$ (right). All intensity values are shown in cps.

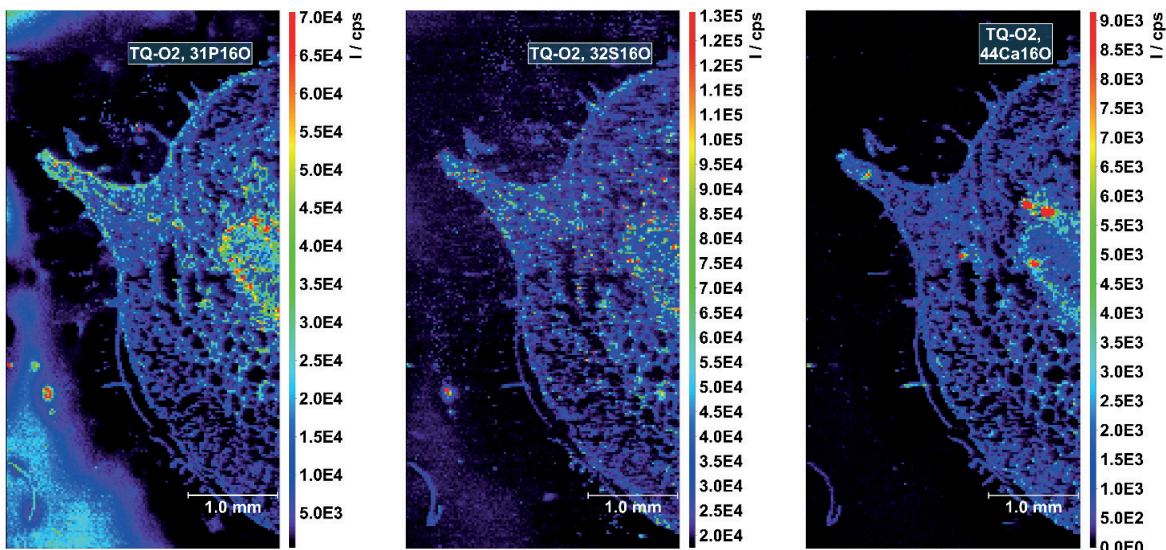


Figure 3. Elemental distribution maps for the TQ-O₂ analysis of ³¹P¹⁶O (left), ³²S¹⁶O (middle) and ⁴⁴Ca¹⁶O (right). All intensity values are shown in cps.

As can be seen in Figure 2 and Figure 3, the mass shift reaction with oxygen successfully removes most interferences for P (Figure 2 and Figure 3, left) and S (Figure 2 and Figure 3, middle) in SQ- and TQ mode. Consequently, the general structure of the petiole cross section can be differentiated from the background very clearly. Noticeably, the embedding medium, which surrounds the sample, is contaminated with high amounts of P, which can be seen in both modes.

For Ca (Figure 2 and Figure 3, right), the mass shift reaction with oxygen itself is not sufficient for effective interference removal. This leads to a blurry image in SQ mode (Figure 2, right) where only the Ca hotspots are clearly visible. Those hotspots correspond to idioblasts, specialized cells that accumulate calcium oxalate as a defense against herbivory. In contrast, when TQ mode is applied, the Ca distribution in the whole section can be visualized, including the finer trichome structures, as the background concentration caused by the interferences is decreased to zero.

Results – Comparison of SQ-O₂ and TQ-O₂ modes for the analysis of rat kidneys

For thin section samples derived from animals, e.g. in clinical research studies, it is common that the distribution of more than just one element is of high interest. Therefore, the mass imaging mode has to be a good compromise between the number of analytes and obtainable sensitivity and spatial resolution. Similar to plant samples, many of the elements of interest are suffering from interferences on their major isotopes, such as iron (e.g., ⁴⁰Ar¹⁶O⁺ on ⁵⁶Fe⁺) or selenium (e.g., ⁴⁰Ar⁴⁰Ar⁺ on ⁸⁰Se⁺).

For comparison of single quadrupole and triple quadrupole performance, two parallel thin sections of a rat kidney have been analyzed in SQ-O₂ (Figure 4 & 5) and TQ-O₂ (Figure 6 & 7) modes. Oxygen has been chosen as a cell gas here to allow mass shift reactions of Se and avoid the strong Ar interferences on mass. Additionally, two parts of the same rat liver thin section (Figure 8) have been analyzed in SQ-KED and TQ-O₂ mode, both highly capable of high interference reduction.

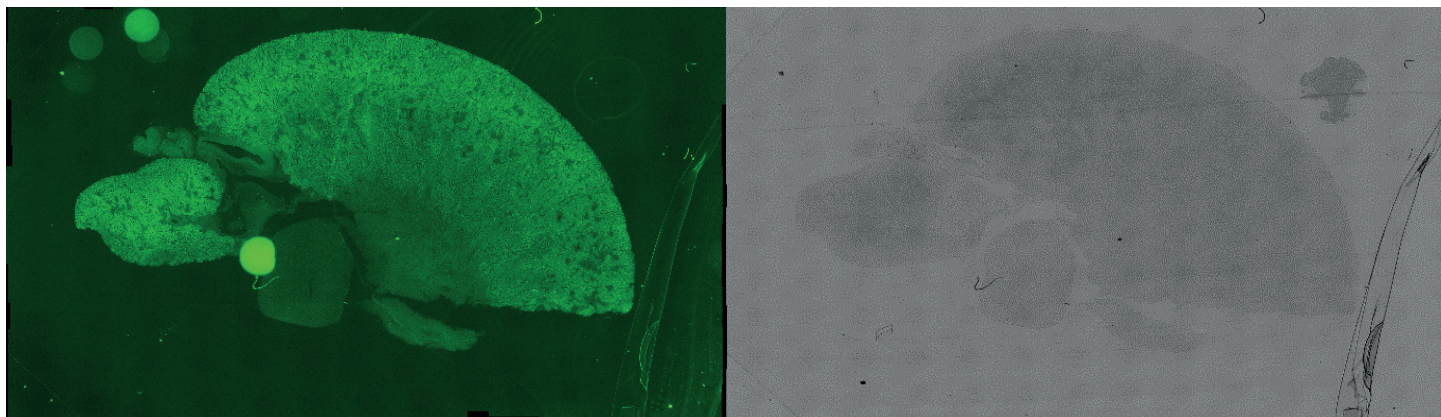


Figure 4. Fluorescence (left) and bright field microscopic image (right) of the rat kidney thin section to be analyzed in SQ-O₂ mode

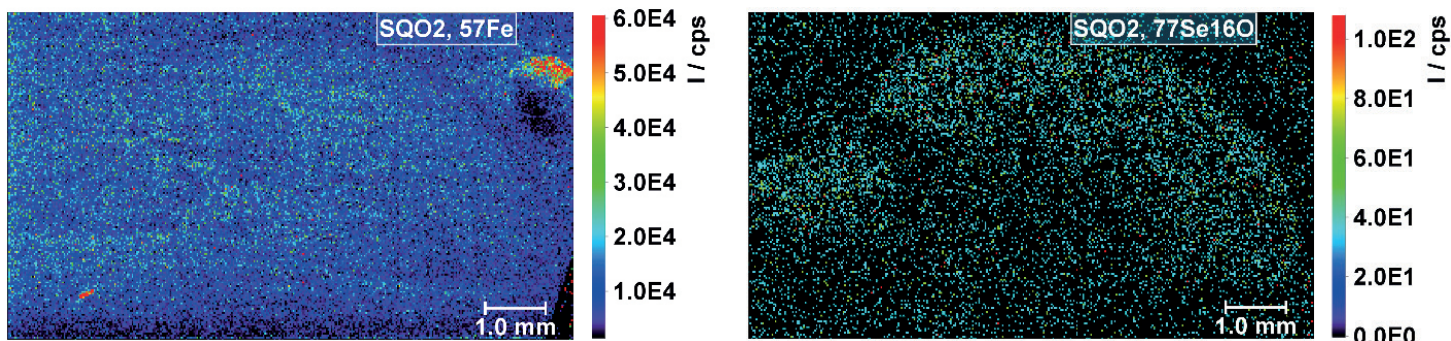


Figure 5. Elemental distribution maps for the SQ-O₂ analysis of ⁵⁷Fe (left) and ⁷⁷Se¹⁶O (right). All intensity values are shown in cps.

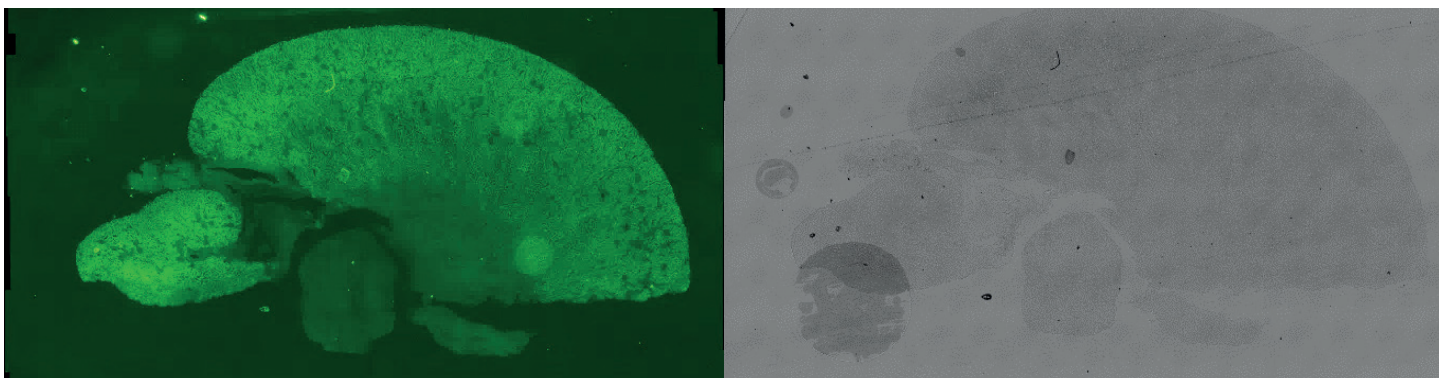


Figure 6. Fluorescence (left) and bright field microscopic image (right) of the rat kidney thin section to be analyzed in TQ-O₂ mode

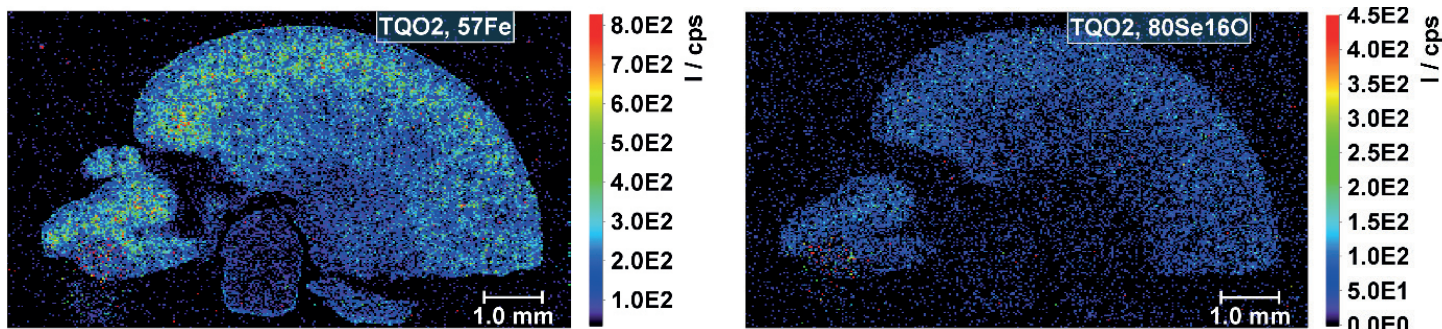


Figure 7. Elemental distribution maps for the TQ-O₂ analysis of ⁵⁷Fe (left) and ⁸⁰Se¹⁶O (right). All intensity values are shown in cps.

As can be seen in Figure 5, neither the Fe nor the Se distributions in the rat kidney thin section are clearly visible in SQ-O₂ mode.

For ⁵⁷Fe (Figure 5, left), the background intensities are still too high due to the formation of ⁴⁰Ar¹⁶O¹H and ⁴⁰Ar¹⁷O in the CRC, so differentiation of background and sample is very difficult to achieve. For ⁷⁷Se¹⁶O (Figure 5, right), the background intensities are close to zero, but the intensities of the minor Se isotope at *m/z* 77 are too low for visualization. The major isotope at *m/z* 80 (not shown here) gives even worse distribution maps due to the strong Ar interferences even after mass shift reactions through formation of ⁹⁶Ar₂O from ⁴⁰Ar⁺ and ⁴⁰Ar¹⁶O⁺ ions.

In contrast to the SQ-O₂ results, the TQ-O₂ mode enables visualization of both Fe and Se distributions (Figure 7). For ⁵⁷Fe (Figure 7, left), the application of the first quadrupole as a mass filter removes the Ar⁺ precursor ions so they cannot react with oxygen in the cell, and therefore lowers the background intensities successfully to reveal the detailed distribution within the sample.

For ⁸⁰Se¹⁶O (Figure 7, right), the intensities are still relatively low due to the minimal amount of Se present in the sample. As the TQ-O₂ mode removes argon based precursor ions, and furthermore the ⁸⁰Ar₂ dimer does not oxidize, effectively all interferences at this *m/z* have been removed. The major isotope of Se can be used in this case (*m/z* 80 with mass shift to *m/z* 96), allowing the Se distribution within the sample to be visualized even at low concentrations.

Results – Comparison of SQ-KED and TQ-O₂ modes for the analysis of rat livers

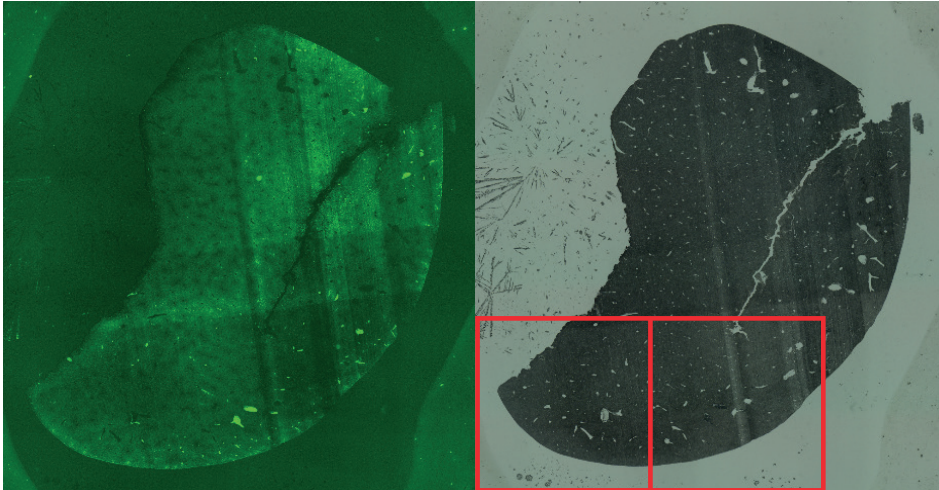


Figure 8. Fluorescence (left) and bright field microscopic image (right) of the rat liver thin section to be analyzed in KED and TQ-O₂ mode. Red rectangles indicate the part analyzed in KED (left) and TQ-O₂ (right) mode.

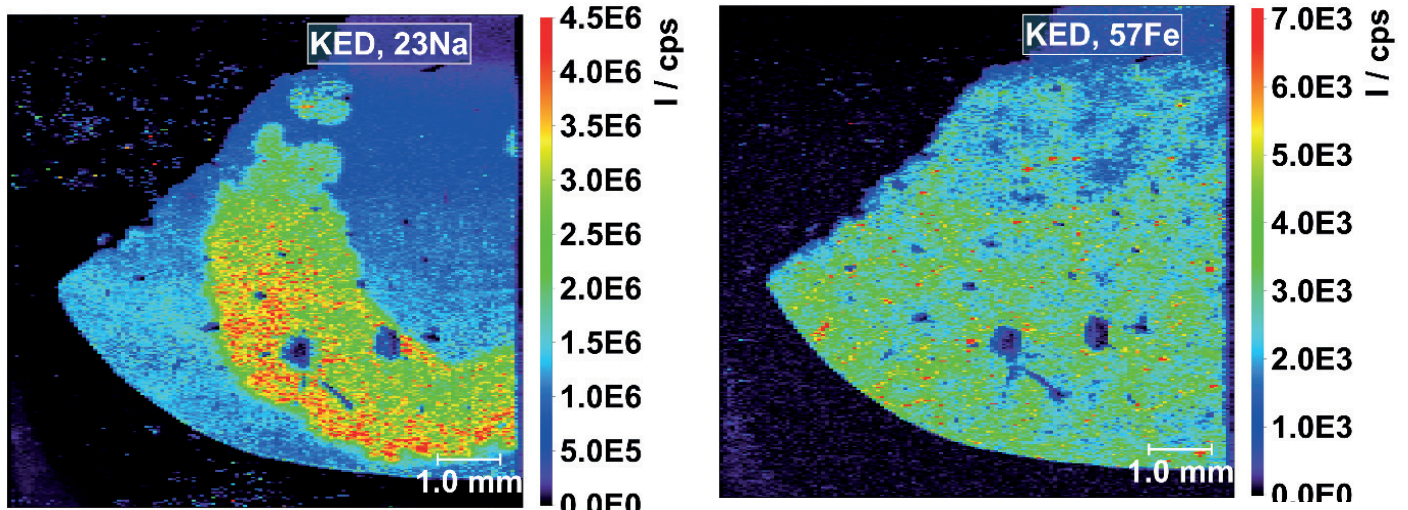


Figure 9. Elemental distribution maps for the SQ-KED analysis of ²³Na (left) and ⁵⁷Fe (right). All intensity values are shown in cps.

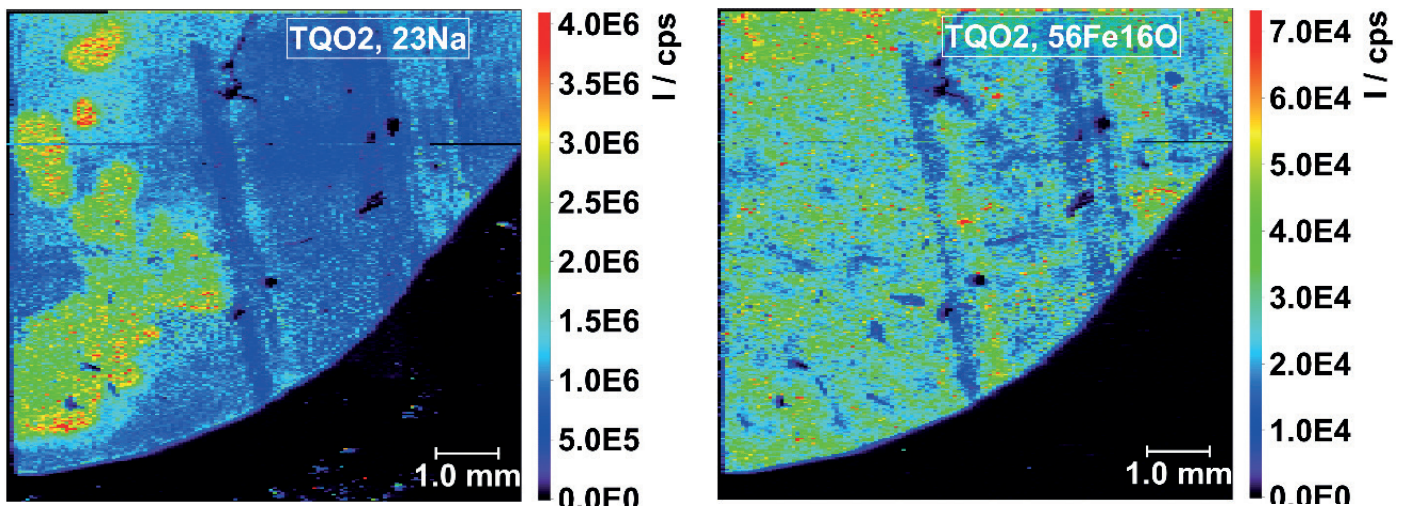


Figure 10. Elemental distribution maps for the TQ-O₂ analysis of ²³Na (left) and ⁵⁶Fe¹⁶O (right). All intensity values are shown in cps.

The Na distribution in the rat liver thin section is clearly visible in both modes, SQ-KED (Figure 9, left) and TQ-O₂ (Figure 10, left) – which is not surprising as Na is not a highly interference burdened element. It is noticeable though that the additional Q1 mass filter applied in TQ mode does not lead to a severe loss of sensitivity as could have been expected (4.5 × 10⁶ cps as a maximum in SQ-KED mode compared to 4.0 × 10⁶ cps as a maximum in TQ-O₂ mode). Therefore, TQ-O₂ is a good compromise when several elements have to be analyzed at the same time, even if not all of them benefit from the interference correction.

The Fe analysis gives similar general distributions in SQ-KED (Figure 9, right) and TQ-O₂ (Figure 10, right) mode. However, the analysis in TQ-O₂ mode can take place on the major Fe isotope (*m/z* 56 shifted to *m/z* 72) while the SQ-KED mode can only eliminate interferences on the minor ⁵⁷Fe isotope. This leads to significantly higher sensitivity in TQ-O₂ mode (7.0 × 10⁴ cps as a maximum) when compared to SQ-KED mode (7.0 × 10³ cps as a maximum). Here, TQ-O₂ has a clear advantage and, coupled with good transmission as is shown with the Na map, a full multi-element map can be obtained using just a single mode on the iCAP TQ ICP-MS, which retains speed and therefore image resolution with optimized interference removal for those elements that require it.

Conclusion

The LA-ICP-MS system described has been shown to be ideally suited for the high spatial resolution bioimaging analysis of various elements in thin sections in both single and triple quadrupole analysis modes. Triple quadrupole technology easily and reproducibly eliminates background spectral interferences on key analytes such as P, S, Ca, Se and Fe in biological samples. The use of triple quadrupole technology in the iCAP TQ ICP-MS system clearly improves the images produced for analytes such as Ca (through the analysis of ⁴⁴Ca¹⁶O at *m/z* 60), iron (through the analysis of ⁵⁶Fe¹⁶O at *m/z* 72) or Se (through the analysis of ⁸⁰Se¹⁶O at *m/z* 96), enabling a wider dynamic range and cleaner backgrounds to reveal additional structural information not detectable by traditional single quadrupole ICP-MS.

Acknowledgments

We would like to acknowledge the contribution of the group of Prof. Antje von Schaewen (Institute of Plant Biology and Biotechnology, University of Münster) in providing the tobacco samples used in this study.

Find out more at thermofisher.com/TQ-ICP-MS

For Research Use Only. Not for use in diagnostic procedures. © 2020 Thermo Fisher Scientific Inc. All rights reserved. Teledyne CETAC Technologies is a trademark of Teledyne Instruments Inc. Technovit® is a registered trademark of Heraeus Kulzer GmbH. All other trademarks are the property of Thermo Fisher Scientific and its subsidiaries. This information is presented as an example of the capabilities of Thermo Fisher Scientific products. It is not intended to encourage use of these products in any manners that might infringe the intellectual property rights of others. Specifications, terms and pricing are subject to change. Not all products are available in all countries. Please consult your local sales representatives for details. Not all products are available in all countries. Please consult your local sales representatives for details. **AN43358-EN 0620C**

ThermoFisher
SCIENTIFIC